IEEE Open Access Journal of
Power and Energy

Received 6 January 2026; revised 28 April 2026; accepted 4 May 2026. Date of publication 7 May 2026; date of current version 13 May 2026.

Digital Object Identifier 10.1109/OAJPE.2026.3691248

The Effects of Summer-Only River Energy on Microgrid-Size Battery Energy Storage at High Latitudes

BAXTER W. BOND (Member, IEEE), LUKE O. WOODHOUSE, PAUL X. DUVOY, NATHAN J. GREEN, AND BENJAMIN H. LOEFFLER

Alaska Center for Energy and Power, University of Alaska Fairbanks (UAF), Fairbanks, AK 99775 USA

CORRESPONDING AUTHOR: B. W. BOND (bwbond@alaska.edu)

This work was supported by U.S. Department of Energy's Office of Energy Efficiency and Renewable Energy (EERE) through the Water Power Technologies Office (WPTO) under Award DE-EE0009445.0000.

ABSTRACT Riverine hydrokinetics (RHK) represent an emerging technology in the renewable energy space with commercially-deployable systems on the horizon. In Alaska, many rural and remote communities exist on major rivers and are burdened by high costs of electricity and imported fuel, making them a promising end-user of these systems. However, it remains an open question as to how the addition of RHK will affect grid performance and electricity costs. Specifically, this study looks at the effects of integrating riverine hydrokinetics on a hybrid diesel microgrid with solar and battery infrastructure. Using real electrical load data and riverbed transects, estimated RHK costs, and modeled solar photovoltaic and river energy resources, a HOMER model was used to analyze the effects on battery degradation, and then expanded to look at fuel usage and levelized cost of energy. The addition of summer-only hydrokinetics was shown to have negligible impacts on battery performance and no impact on battery lifetime. Fuel savings were proportional to RHK size at lower penetrations, but diminished at higher penetrations due to significant curtailment. The estimated capital and operational costs of the RHK predicted an increase in LCOE for all scenarios, ranging from 16% to 39% with increasing system size.

INDEX TERMS Microgrids, river hydrokinetic energy, energy storage, battery degradation.

NOMENCLATURE

Abbreviation	Expansion
ADCP	Acoustic Doppler current profiler.
ASM	Advanced Storage Module.
BESS	Battery energy storage system.
CapEx	Capital expenditures.
DOD	Depth of discharge.
EOL	End of life.
HOMER	Hybrid Optimization of Multiple Energy Resources.
IEA	International Energy Agency.
kW	Kilowatt.
kWh	Kilowatt-hour.
LCOE	Levelized cost of electricity.
MW	Megawatt.
MWh	Megawatt-hour.
NLR	National Laboratory of the Rockies.
O&M	Operations and maintenance cost(s).
PCE	Power Cost Equalization.
PV	Photovoltaic.
RHK	Riverine hydrokinetic.
SOC	State of charge.
TMY	Typical meteorological year.
VRE	Variable renewable energy.

I. INTRODUCTION

A. RENEWABLE ENERGY IN ALASKAN MICROGRIDS

ABOUT a fourth of Alaska's population resides outside of the central electrical grid known as the "railbelt", [1] living in standalone microgrids that are dominated by diesel electricity generation [2]. The energy burden, described as the ratio of a household's energy costs to household income, is extreme among this population: between 2013 and 2018 the mean household energy burden across the Yukon-Koyukuk and the Southwestern census areas all exceeded 10%, compared to an average of 2.5% in the

lower 48 states [3]. The range of electrical rates in rural communities are three to five times higher than the average $0.191/kWh rate in Anchorage, Fairbanks, and Juneau in 2018 [4]. As of 2024, 188 Alaskan communities participated in the state's Power Cost Equalization (PCE) program, but despite the subsidy the weighted average cost of electricity for residents remained $0.2628/kWh, ten cents above the national average [5], [6].

The substantial energy cost burden in rural Alaska has led to an interest in alternative energy production. Wind, solar and hydro-electric projects have become increasingly prevalent, with 31 PCE communities reporting renewable energy generation in 2024 [5]. These projects have the dual ambition of driving down energy costs as well as boosting energy independence by creating local jobs and reducing reliance on PCE. Figure 1 illustrates the increase in wind and solar generation among PCE recipients over the last two decades.

In 2024, the International Energy Agency (IEA) created a framework identifying 6 phases of variable renewable energy (VRE) integration into grid systems [7]. The incentive behind this was to categorize the challenges associated with the uptake of VRE within each phase and give a targeted approach for utilities to address these issues. Phases 1 to 3 entail relatively low-cost modifications to address integration, whereas the higher phases require marked changes in system structure to maintain power quality. Due to the nature of their grid sizes, many Alaskan communities are already reaching phases 3 or 4 of the six-step framework, raising concerns over VRE effects on power quality and grid reliability [8], [9].

For systems in the higher phases, IEA cites various methods for grid management including energy exports, various duration storage solutions, demand response and curtailment. The remoteness of Alaskan microgrids and their limited human capital and infrastructure make many of the conventional solutions unattainable. Nevertheless a variety of integration strategies have been adopted across the state [8]. In particular, recent improvements to inverter technologies have made battery energy storage systems (BESS) with grid-forming inverters feasible for the first time in these microgrids [9], and preliminary studies have shown promise for their continued adoption [10].

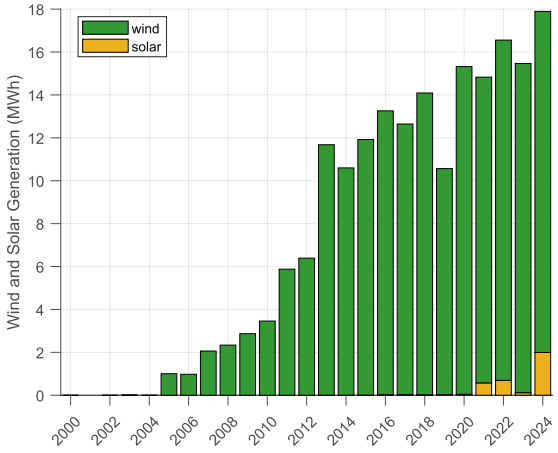

FIGURE 1. Total wind and solar generation across PCE communities between the year 2000 to 2024 [5].

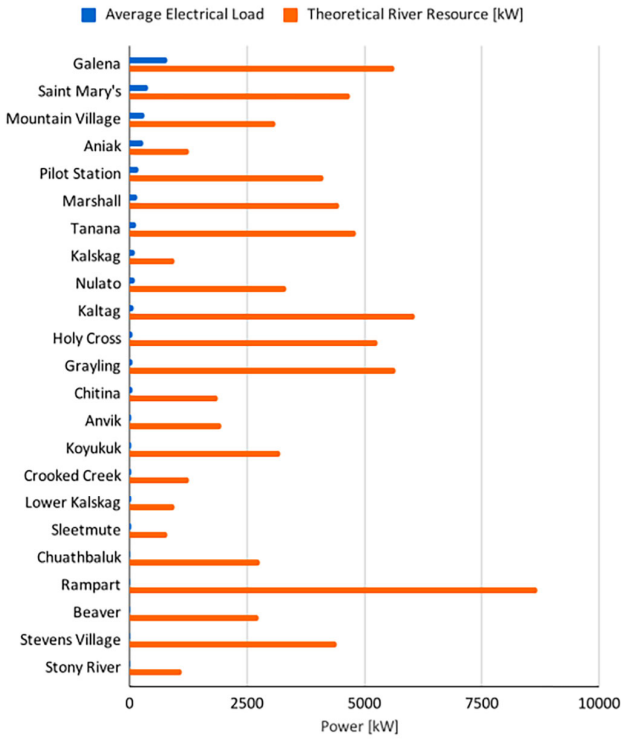

FIGURE 2. Alaska river communities with their load and river energy resource [12], [13].

B. RIVERINE HYDROKINETICS

An untapped energy resource presents itself by virtue of many Alaskan communities proximity to major rivers where traditional hydroelectric plants are infeasible. While the field of riverine hydrokinetics (RHK) is relatively nascent [11], a survey in 2024 of Alaskan riverine communities suggests there is a high capacity for power supply, shown in Figure 2 [12], [13].

The majority of these riverine communities exist in Interior Alaska where wind and traditional hydro resources are scarce [14]. Thus many of the alternative energy projects that are developing in the Interior involve solar photovoltaics (PV) as the economical renewable energy source and BESS with grid forming inverters to provide energy arbitrage and periods of diesels-off operation. If the trend of these installations is projected to continue, it is logical that solar and BESS should be included in future modeling efforts of Interior Alaskan microgrid systems.

A community that is perhaps the most emblematic of these energy transitions in the Interior is Galena, along the

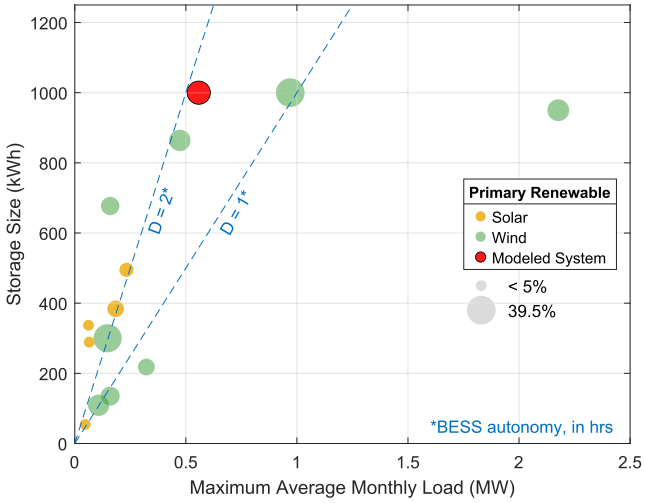

FIGURE 3. Nameplate capacity of currently operating BESS installations in Alaskan microgrids, relative to maximum average monthly load as reported by PCE 2024. Point size is proportional to combined wind and solar penetration level. The dashed lines give a reference battery "duration", defined in hours at the maximum average monthly load.

Yukon River in Alaska's western Central Interior with a population of 435 [5]. As of writing, Galena is constructing a 1.5 MW solar array and a 1 MWh BESS. The size of the solar array farm is comparable to the peak load of the community, thus propelling itself directly into a phase 4 grid by IEA's framework. Figure 3 shows that while it is among the upper echelon of BESS adopters across the state, it follows the general trend in sizing its energy storage relative to the community load. To position this study to be the most timely and representative for future Alaskan microgrids, Galena was chosen as a representative case study for understanding the techno-economic effects of RHK assets on solar-BESS dominated microgrids. While it is on the larger side of the communities under consideration in terms of load, solar capacity and BESS size, all of these factors are currently on the rise. Thus Galena serves as a reasonable approximation for future communities. Furthermore, many of the results are prescribed by the *ratio* of VRE to load, which can more easily be extrapolated to communities of differing sizes.

Given the challenges surrounding high-penetrating integration of renewables, the addition of any new resource needs to be preceded by substantial modeling on grid effects and services. Prior studies on RHK turbine deployment in microgrids include [15] and [16]. However, these are in tropical climates where the resource is available year round. Many Alaskan rivers freeze for long periods of time during the winter, necessitating summer-only deployments. In this study, the impacts of summer-only riverine energy on the levelized cost of electricity (LCOE) and battery performance of the representative community were examined. The focus was on power exploration rather than physical and logistical limitations, in hopes of better understanding the energy balance phenomena at play. This has the dual purpose of informing grid operational decisions to help improve system compatibility as well as to size RHK systems for optimal performance. These results will help any community or utility to better understand the costs and benefits associated with a potential hydrokinetic project, and will also help to inform future research directives.

II. METHODS

The Hybrid Optimization of Multiple Energy Resources (HOMER) software, originally developed by the National Laboratory of the Rockies (NLR) and now developed by UL Solutions, was selected as the modeling suite. This software has been used extensively in prior research on hybrid diesel microgrids [15], [17], [18], [19], [20], [21]. Included in the suite is the Advanced Storage Module (ASM), which estimates battery degradation using rate-dependent losses, the rainflow-counting algorithm and temperature effects [22]. The rainflow-counting algorithm is commonly used to more accurately model battery lifetime [23], [24].

A. ENERGY & INFRASTRUCTURE

To best approximate the diesel generation in HOMER, publicly available information from Rural Alaska Communities Energy Efficiency profiles provided by the Alaska Energy Authority [4] was utilized alongside communication with the powerhouse engineering contractor in Galena. The following diesel generators were used in the model: a Caterpillar 1010 kW, a Caterpillar 450 kW, a Caterpillar 600 kW, and two Kohler 360 kW.

Minutely load data from 2022 to 2024 was provided by the community utility and was downsampled to hourly resolution. Downsampling was either a simple mean over the course of the hour, or the median value in the case of an outage. 2023 was chosen as the representative year because it had fewer gaps than the neighboring years. Gaps were filled from 2024 due to the majority of the available data from 2022 not aligning with missing values. Any remaining gaps were filled from the previous week at the same hour of day.

The battery used in the simulation is a generic 1 kWh lithium ion battery available within the ASM. Based on communication with the contractor selected for the solar energy and battery storage project, the BESS was sized to 1080 DC volts, 4 parallel strings, and 1.2 MWh capacity in HOMER. To accurately account for the cumulative effects of battery degradation, the project lifetime was selected to be 20 years, which is longer than even the most conservative rated lifetime of li-ion BESS systems [25], [26].

In order to model PV output, typical meteorological year (TMY) data was downloaded from the PhotoVoltaic Geographic Information System provided by the European Commission [27]. Galena's TMY is based on the ERA5

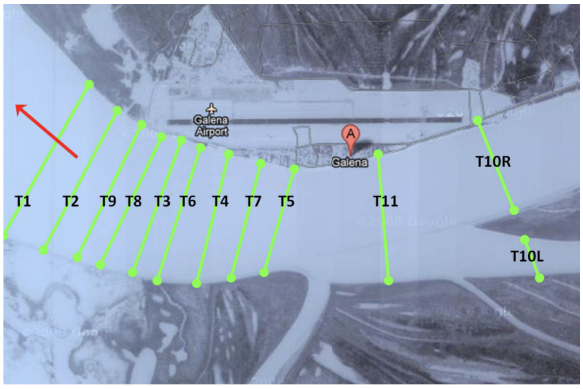

FIGURE 4. Satellite image showing the location of transect T10R in Galena, AK. Figure from University of Alaska Anchorage [30].

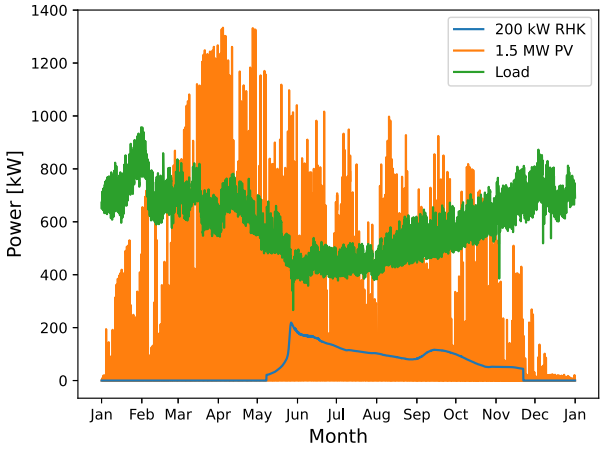

FIGURE 5. Comparison between load and resource availability.

reanalysis data from the European Center for Medium Range Weather Forecasting and built by the ISO 15927-4 procedure [27], [28]. The TMY were then fed into the System Advisor Model developed by NLR. The Perez sky diffuse model was used, and the monthly ground albedo values set at 0.8 for months with snow (October through April) and 0.2 for the months without snow [29]. The ground coverage ratio was set at 0.36 from conversations with the contractor. For the subarrays, 24 of 550 watt modules were used. The overall array was sized to be 100 subarrays in parallel. Twelve 125 kVA inverters were selected, for an overall rating of 1500 kW. This is similar to the array in construction for the community.

The individual RHK turbine was sized to 100 kW nameplate capacity at a rated speed of 2 m/s. Through linear combination of this turbine, a large range of RHK electrical capacity was explored. Water flow velocity was calculated from data originally acquired with acoustic doppler current profiler (ADCP) transects by a field crew from the University of Alaska Anchorage [30], who established power relationships between stream discharge and depth-averaged velocity at specific measurement points. Using these regression equations, average and maximum flow velocities were calculated for transect T10R in Figure 4 based on USGS discharge data from 2020 to 2024 [31]. The theoretical river resource from the year 2023 was used to match the load data. Transect T10R was identified as a potential location for RHK deployment based on the ADCP velocity measurements obtained during the original survey. Only data from the open water season were considered, defined as May 1st through November 15th for this analysis. Figure 5 plots the available resource in the modeled year for an example 200 kW RHK system along with PV and community load data.

Long term river resource was not considered. Reference [32] determined that the average discharge for the middle and upper Yukon river basins have decreased since 1984 by a small but statistically significant amount. Galena is located in the middle basin, so long term river resource is expected to reduce slightly.

B. BATTERY DYNAMICS

The lithium-ion batteries were modeled using HOMER's Modified Kinetic Battery Model for an assessment of their performance and lifetime. This model takes into account a number of factors affecting battery life, including rate-dependent losses, temperature effects, and cycling [33]. HOMER separates these factors into two "variables", grouping calendar and temperature effects into one, and cycling adjusted for depth-of-discharge as the other. Due to irregularities in battery cycling with VRE, a "Rainflow Counting" algorithm is used to convert state of charge time series into cycle-equivalent depth-of-discharge (DOD) [22]. The number of cycles and their associated DOD is then used to calculate cycling degradation.

In general, battery degradation manifests in two ways: as a loss in battery capacity or an increase in internal battery resistance [34]. An empirical model described by [35] and used in HOMER's ASM assumes that cell resistance growth is an additive effect of the two variables, calendar and temperature effects and cycling, whereas capacity losses are controlled by the largest of the two. Thus the end of life (EOL) criterion for a battery depends on whether series resistance or capacity loss is the limiting factor, which varies depending on the use case. These two metrics are strongly interrelated, but capacity loss typically has a stronger correlation with battery lifetime [36] and is easier to predict [37], so it was used in this study. Beyond EOL calculations, HOMER does not account for the effect of increased series resistance on round-trip efficiency, but it does factor in capacity losses on the DOD during cycling.

A summary of the battery specifications used in HOMER are provided in Table 1. The contractor provided a degradation curve and an EOL estimate of 5000 cycles from preliminary equipment quotes, from which the capacity degradation limit of 65% was chosen. The minimum state of charge was set to 35%.

TABLE 1. Lithium-Ion BESS specifications.

Total cells	1168
Nominal voltage (VDC)	1,080.4
Nominal capacity (kWh)	1,191.3
Maximum capacity (Ah)	1,104
AC & heating load (kWh/day)	0-50*
Initial SOC (%)	35
Minimum SOC (%)	35
Replacement degradation limit (%)	65
Capital	$1,101,400
Annual O&M	$11,680

∗: Not used in simulation

Due to temperature control on the BESS enclosures, temperature effects were not considered in this analysis. Reference [38] estimates that the daily BESS temperature control loads for an insulated containerized system in Fairbanks range from 0 kWh to 50 kWh, which is negligible compared to the peak daily community demand of 19.2 MWh. Fairbanks experiences a similar climate to Galena [39], so the heating needs are expected to be similar.

C. ECONOMICS

Cost estimates used are taken from a range of years, so they were converted to a standard dollar-year using the consumer price index (CPI) [42]. For each component, the associated annual national CPI for its year was used to convert to 2023 dollars [43].

The cost of diesel generators depend on their size. Reference [2] was used to estimate the capital and operating costs by generator size. The cost curve estimates were used to find the capital costs in 2014 dollars and then converted to 2023 dollars. Operating and maintenance costs were done identically. Replacement cost is estimated to be $700/kW. Diesel fuel costs are $4.24 per gallon or $1.12 per liter in 2023 dollars [5]. See Table 2 for complete cost estimates.

Due to it's nascent state, accurate cost estimates for hydrokinetics are hard to come by. Sandia National Lab's dual rotor Reference Model 2 (RM2) provides the most extensively-researched source of these estimates and was therefore used for this study [40]. Nameplate capacity is 50 kW for each RM2 rotor, for a total of 100 kW. Capital costs come from environmental permitting, installation of moorings and turbines, structural material, and electronics, while replacement costs omits the permitting costs. The economies of scale from 1 to 10 units are considered. The original values were in 2014 dollars and were converted to 2023 dollars.

The BESS capital cost was assumed to be $1000 per kWh [18], although estimates for lithium ion BESS in rural Alaskan communities vary widely, from as low as $400 per kWh [44] to $10,000 per kWh [45]. As of writing, replacement costs are unknown, but if set too high they can cause HOMER's modeled dispatch strategy to bypass using the battery entirely. For this model it was assumed to be $600 per kWh, and it was found that lowering this cost has minimal effect on LCOE estimation and does not affect battery usage.

Like BESS, solar costs in Alaska vary widely depending on the geographic location of the array. As a state, the cost of a solar array varies from $1.25/W to $4.60/W in 2018 dollars, depending on remoteness and size [41]. As of writing, a large 1.5 MW solar project has not been completed in rural Alaska, so the associated costs are unknown. The large size of the array favors economies of scale, but this is counterbalanced by the remoteness of the location. A CapEx of $1.90/W in 2018 dollars was chosen, which corresponds to $2.33/W in 2023. O&M costs vary as much as capital [41]. $66/year in 2023 dollars was chosen based on Galena being a larger village but not connected to the road system.

III. RESULTS AND DISCUSSION

A. MODEL VALIDATION

To validate the HOMER model, the diesel only scenario was compared to PCE reporting for state fiscal year 2023 and 2024. The model predicted 5291 MWh of diesel generation, whereas PCE reported 5,116 MWh of generation in 2023 and 5,331 MWh in 2024 [5], [13]. This is between a 3.4% and a 0.75% difference. The modeled annual fuel usage was 357,473 gallons, while the reported values for state fiscal year 2023 and 2024 were 375,653 and 368,393 gallons, respectively. Therefore the model roughly gives a 3% to 4.8% underestimate on fuel usage. This is less than the year to year variability of consumption of the community from 2012 to 2021 [46]. Because HOMER utilizes economic dispatch, which is not often practiced in rural communities in Alaska, this could represent possible savings in dispatch and should not affect overall conclusions.

Explanations for model deviations from the real system include differences in real versus modeled generator fuel curves and generator dispatch, PCE reporting timing, and powerhouse load losses. The model uses the generators sizes listed above in Table 2 while the sizes of the actual generators deployed are two 370 kW, and one each of 455 kW, 600 kW, and 1050 kW. PCE reporting is from July to June, while HOMER uses the calendar year, so there is inherent mismatch in the comparison. Finally, the load data provided was gathered at the feeder, rather than the generator. Therefore, it does not include powerhouse loads, and represents the community-only load with line losses.

B. EFFECTS ON BATTERY PERFORMANCE

To better contextualize the effects of hydrokinetics on battery performance, a sensitivity analysis was conducted with different system architectures. The results of this analysis are shown in Figure 6. Three variables were scaled independently from one another: battery storage capacity (kWh), PV nameplate (kW), and RHK nameplate (kW), with annual battery throughput as the dependent variable. During the scaling of each variable, the other two were held constant,

TABLE 2. Economics of infrastructure in 2023 dollars.

Item	CapEx	O&M	Replacement	Lifetime	Source
Diesel gen., 360 kW	$2,149,000	$64.34 per hr	$257,000	70,000 hrs	[2]
Diesel gen., 450 kW	$2,316,000	$53.61 per hr	$322,000	70,000 hrs	[2]
Diesel gen., 600 kW	$3,166,000	$57.19 per hr	$429,000	70,000 hrs	[2]
Diesel gen., 1010 kW	$3,249,000	$59.57 per hr	$722,000	90,000 hrs	[2]
RHK, 1x100 kW	$2,970,000	$260,000 per yr	$2,140,000	20 yrs	[40]
RHK, 10x100 kW	$9,720,000	$700,000 per yr	$8,000,000	20 yrs	[40]
BESS	$1,000 per kWh	$10 per yr kWh*	$600 per kWh	65% cap.	[18]
Solar PV	$2.33 per W	$66 per yr	$1.50 per W†	20 yrs	[41]

∗: HOMER default

†: Assuming replacement cost is 65% of capital

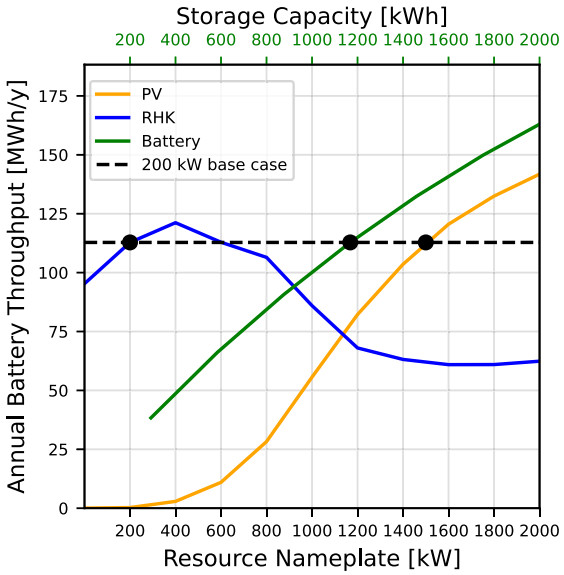

FIGURE 6. Effects of scaling resource nameplate and storage capacity on annual battery throughput by holding two variables constant.

with the reference being a 1.2 MWh BESS, 1.5 kW PV array, and 200 kW RHK system. The initial target point of 200 kW RHK was chosen as a likely upper bound on nameplate capacity for an achievable riverine hydrokinetic pilot project. Throughput was used as an easily-quantifiable metric for battery usage, roughly indicative of degradation rates.

Figure 6 shows that battery throughput is positively correlated to solar and battery size, with roughly a linear relationship near the reference point. In contrast, the throughput's dependence on RHK nameplate is unimodal, reaching an apex at 400 kW. Unlike other renewables, RHK has relatively steady production on a day-to-day basis, and thus when the resource exceeds the load, 600 kW RHK and above, the grid is able to run diesels off without use of the battery for extended periods of time. This leads to a decrease in annual throughput.

It is evident from Figure 6 that several unique operational regimes exist for the battery based on the size of RHK:

TABLE 3. Predicted battery behavior for various RHK.

System	Annual Throughput	Replacement Year
No RHK	95,301 kWh	18
200 kW RHK	112,811 kWh	18
400 kW RHK	121,183 kWh	18
1,000 kW RHK	85,973 kWh	18

low penetrations with no diesels off, high penetrations *with* diesels off, and an intermediate region that sees the most battery cycling. To better understand each of these regimes, the following system architectures were chosen for further analysis: a control of 0 kW, the reference case of 200 kW, the system that yielded the highest throughput, 400 kW, and an extreme case of 1000 kW.

Basic lifetime performance metrics for the battery under these four cases are provided in Table 3. For every case the predicted battery lifetime is 18 years. This is relatively long compared to typical BESS lifetimes, but is reasonable when considering that little to no cycling occurs for half of the year. The independence of this result from system size suggests that even in the most extreme case at 400 kW RHK, there is not enough cycling occurring to degrade the battery faster than its background time degradation rate. Conferring Figure 6, it can be deduced that on top of this base system architecture, no penetration of RHK would change the estimated battery lifetime.

Figure 7 tracks the aggregated battery degradation for all four cases across a deployment season, as predicted by the ASM. Time degradation is also included in this plot, which is defined as a flat rate in HOMER and is equivalent for all four cases. As expected, the cycling-induced degradation falls short of the time degradation under all system architectures.

Looking more closely, each system experiences periods of time in which the battery cycling is greatly reduced or stopped entirely, suggesting the battery is either at a minimum or maximum state of charge (SOC). For the base case with PV only, gaps in solar resource overnight make it impossible for the battery to be held at a full SOC, so these are clearly periods of depleted storage. For the other three

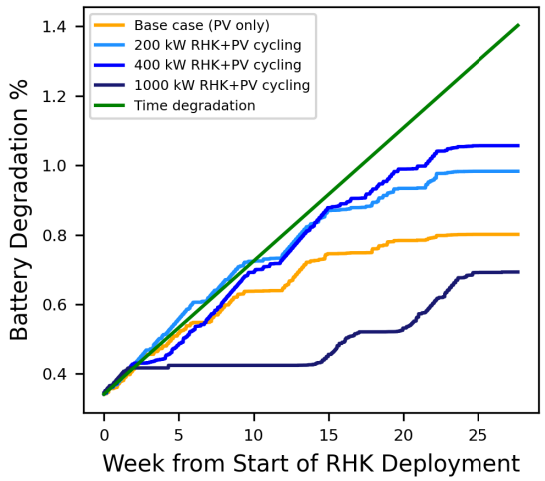

FIGURE 7. **Degradation due to calendar wear and battery cycling plotted as a % increase from the start of RHK deployment.**

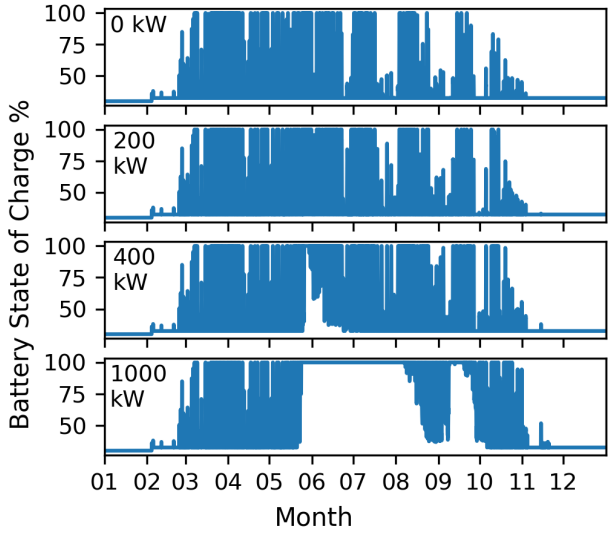

FIGURE 8. **Battery SOC in a calendar year for various levels of RHK.**

cases, extended periods without cycling that are not mirrored in the base case must then reflect a maximum SOC. This is ultimately the driver behind the decreased annual throughput seen at higher penetrations of RHK in Figure 6. To confirm this, Figure 8 presents time series plots of the battery SOC.

While excess hydrokinetic resource explains the periods of reduced cycling, heightened degradation rates are seen during other periods of the year in the same systems. The source behind this is not immediately evident in the SOC plots, so two periods of interest were chosen for a more detailed time series analysis: May 20th - 26th, and August 25th - 31st.

In May, the PV resource is generally high, and the riverine resource is increasing with spring melt. RHK output reaches its peak on May 27th, which can be seen in Figure 5.

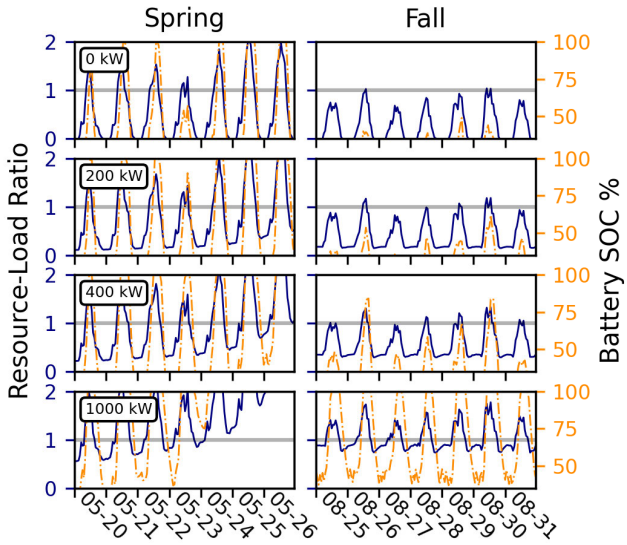

FIGURE 9. **A time series analyses of weeks of high battery use in spring and fall.**

Figure 9 shows that during this time the addition of 200 and 400 kW RHK allows the battery to reach a full state of charge for a longer period during the day, and gives a slightly larger DOD than PV alone. In contrast, the 1,000 kW RHK achieves a state of continuous full charge, as the RHK resource surpasses the community load starting on the 24th. This matches the flattening of the degradation curve on the left end of Figure 7, near week two.

In contrast, August is marked by a lower average PV and riverine resource. Figure 9 in the fall shows that the PV alone generates minimal cycling of the battery, explaining the flattening of the curve in Figure 7 around week 16. With the addition of 200 and 400 kW RHK, the average resource-load ratio is still below the community load, but the DOD is heightened. With 1,000 kW RHK, a full DOD battery cycling occurs every day, with the RHK resource supplying slightly less than the community load and solar periodically increasing total generation across the 1:1 ratio line.

This plot also reveals another counterintuitive process: the battery will begin cycling *before* the resource surpasses the load. For instance, on the 28th and 29th of August, the PV only scenario experiences battery cycling even though the resource never exceeds the demand. This phenomena is also present in May, but is less obvious. Upon further analysis, the premature cycling occurs when the difference between the load and the renewable energy resource is below the minimum power output of the diesel generation. In these circumstances, a typical generation control scheme will cycle on the smallest generator available, but the remaining excess generation will begin a charge cycle on the battery. This is also present in the 1,000 kW RHK system architecture, where slight fluctuations in the battery SOC overnight are observed. This results in the highest rates of observed battery degradation.

TABLE 4. Fuel and costs parameters by RHK size in kW, in reference to base case.

RHK kW	Gallons/ yr	Gal. displ.	LCOE/ kWh	Δ% LCOE	RHK OC%R
0	274,200	-	$0.504	-	-
100	260,500	13,700	$0.585	16.1%	87%
200	247,200	27,000	$0.594	17.9%	79%
400	222,900	51,300	$0.614	21.8%	71%
800	190,500	83,700	$0.667	32.3%	69%
1000	181,100	93,100	$0.700	38.9%	70%

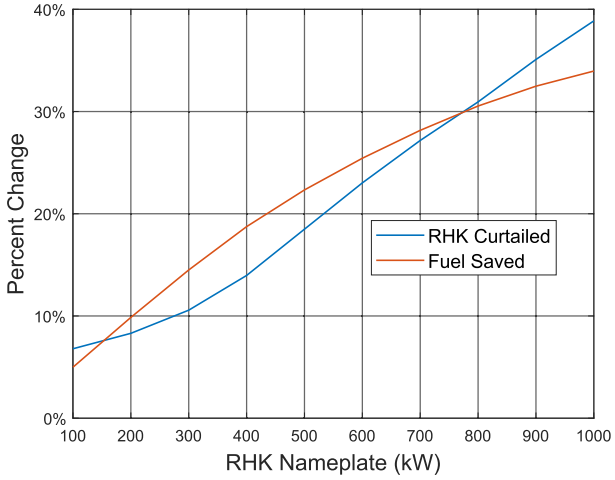

FIGURE 10. % fuel saved vs. % RHK curtailed, base capacity factor of 0.265.

Generalizing, it's clear that the highest throughput occurs when the hydrokinetic resource is just short of the community load, allowing for daily swings in solar and auxiliary diesel to charge and discharge the battery fully. Heightened throughput can be seen as a greater return on battery investment; however this would be more complicated if the battery lifetime was being reduced via cycling.

C. FUEL SAVINGS AND LCOE

Upon the determination that RHK had negligible effects on any of the battery metrics accessible in HOMER, an additional analysis was done on the overall system economics, primarily looking at fuel savings and levelized cost of energy (LCOE). Table 4 presents displaced fuel and LCOE as both a number and percent change. It also presents a cost percent reduction value, or the reduction needed in capital, replacement, and O&M costs of RHK to break even with the base case LCOE.

The addition of RHK increases fuel displacement, but this effect is diminished at higher penetration levels as the grid becomes saturated with the resource and more RHK is curtailed. Figure 10 shows that at 1000 kW RHK, nearly 40% of the river energy is curtailed. The high estimated costs for RHK installation, O&M, and replacement produce a steep and undesirable effect on LCOE. However, the effects of economies of scale are apparent, with a single 100 kW RHK installation needing an 87% reduction in costs to have the same LCOE as the base case, compared to the roughly 70% cost reduction for the 500 to 800 kW size.

IV. CONCLUSION

This study looked at the effects of adding summer-only riverine hydrokinetics to a mid-sized Alaskan microgrid with a 1.5 MW PV array and 1.2 MWh BESS. The base case of a hybrid diesel-PV-BESS system was chosen to provide the most relevance to future Alaskan communities. The results are relevant for any winter-peaking community with high penetration of solar and a similar climate region to Interior Alaska. RHK was implemented at a variety of capacity levels, and the effects on battery lifetime, fuel displacement, and LCOE were explored.

For all of the scenarios in the study, battery lifetime is dominated by calendar degradation and remains unchanged from the base case under different cycling scenarios. Battery throughput and thus cycling degradation at first increases with added RHK and then decreases to below the base case throughput, as VRE reaches high levels of penetration. The peak throughput occurs around 400 kW RHK when the average daily resource hovers close to the community load. In this case the PV supplies nearly a full charge cycle each day, but the RHK is not sufficient by itself to keep the battery topped off. While the additional cycling does not change the predicted battery lifetime, in practice it would increase the battery's internal series resistance and lead to some loss in battery efficiency. Predicting the severity of these losses is beyond the capabilities of HOMER's modeling suite. On the other hand, maximizing throughput can be considered a greater return-on-investment for the battery.

The high modeled cost of RHK is seen to drive a sharp increase in LCOE from the base case, no matter what scale of integration. As one might predict, fuel savings are proportional to the level of RHK added, but the benefit of fuel savings begins to diminish at higher penetrations with more curtailed energy. In contrast, higher penetrations benefit modestly from the economies of scale, and the cost percent reduction value decreases to a minimum of 69% for systems in the range of 600 - 900 kW. Communities of smaller size would predictably benefit less from these economies of scale, and vice-versa. For all of these cases the LCOE remains between 16% to 39% higher than the base case, and increases with the RHK size. For instance a system with 200 kW RHK would require a net reduction in CapEx and O&M $2,918,000 and $154,000 per year, respectively, to break even with the base case.

The modeling suggests that remote, high latitude communities considering adding riverine hydrokinetics to a microgrid should evaluate their specific combination of load, solar and storage. RHK is not predicted to meaningfully extend or degrade BESS life. Therefore, communities should seek to find an optimal capacity of RHK to install that maximizes diesel offset for a given load profile and combination of existing generation, storage assets, and seasonal behavior

while balancing LCOE considerations, especially for new technology.

Areas for future research are substantial. HOMER is an excellent tool for energy balance modeling, but does little to predict the grid instabilities that become a concern at high penetrations of VRE. Future work is planned to address this using a dynamic grid modeling platform. Furthermore, characterization of the under-ice resource potential for RHK penetration year-round would be predicted to substantially change the economics surrounding this report. And finally, replicating this modeling effort with different communities would help to better generalize the results across Alaska.

ACKNOWLEDGMENT

This article was prepared as an account of work sponsored by an agency of U.S. Government. Neither U.S. Government nor any agency thereof, nor any of their employees, makes any warranty, express or implied, or assumes any legal liability or responsibility for the accuracy, completeness, or usefulness of any information, apparatus, product, or process disclosed, or represents that its use would not infringe privately owned rights. Reference herein to any specific commercial product, process, or service by trade name, trademark, manufacturer, or otherwise does not necessarily constitute or imply its endorsement, recommendation, or favoring by the United States Government or any agency thereof. The views and opinions of authors expressed herein do not necessarily state or reflect those of U.S. Government or any agency thereof.

REFERENCES

[1] K. Adediran. *What is the Railbelt?*. Accessed: Jul. 10, 2025. [Online]. Available: https://storymaps.arcgis.com/stories/5311a23d5b7c46cdae3e622fb6961e14

[2] N. Green, M. Mueller-Stoffels, and E. Whitney, "An Alaska case study: Diesel generator technologies," *J. Renew. Sustain. Energy*, vol. 9, no. 6, Nov. 2017, Art. no. 061701, doi: 10.1063/1.4986585.

[3] B. Boettger et al., "Energy burden in Alaska: Understanding energy burden for Alaska communities and charting a path forward," Cook Inletkeeper, Homer, Alaska, Tech. Rep. 1, 2025.

[4] *RACEE Profiles*. Accessed: Jul. 15, 2025. [Online]. Available: https://public.tableau.com/app/profile/alaska.energy.authority/viz/RACEEProfiles/Generalcommunityinformation

[5] *Power Cost Equalization Statistical Report FY2024*. Accessed: Sep. 23, 2025. [Online]. Available: https://www.akenergyauthority.org/LinkClick.aspx?fileticket=PUG4bLWTJDiwa4uX1S45g%3d%3d&portalid=0

[6] *U.s. Energy Information Administration—EIA–Independent Statistics and Analysis*. Accessed: Oct. 28, 2025. [Online]. Available: https://www.eia.gov/totalenergy/data/browser/index.php?tbl=T09.08#/?f=A&start=200001

[7] *Integrating Solar and Wind: Global Experience and Emerging Challenges*. Accessed: Sep. 23, 2025. [Online]. Available: https://www.iea.org/reports/integrating-solar-and-wind

[8] G. P. Holdmann, R. W. Wies, and J. B. Vandermeer, "Renewable energy integration in Alaska's remote islanded microgrids: Economic drivers, technical strategies, technological niche development, and policy implications," *Proc. IEEE*, vol. 107, no. 9, pp. 1820–1837, Sep. 2019.

[9] R. Meadows, E. Edgerly, R. Jordan, and L. Beshilas. *Renewable Energy Integration in Remote Alaska Communities*. Accessed: Sep. 23, 2025. [Online]. Available: https://www.osti.gov/biblio/2522802

[10] J. Flicker, J. Hernandez-Alvidrez, M. Shirazi, J. Vandermeer, and W. Thomson, "Grid forming inverters for spinning reserve in hybrid diesel microgrids," in *Proc. IEEE Power Energy Soc. Gen. Meeting (PESGM)*, Aug. 2020, pp. 1–5.

[11] P. Malali, Z. Ding, and M. A. Villavicencio, "Technology readiness level assessment of hydrokinetic energy converters," *Energy Rep.*, vol. 14, pp. 1240–1250, Dec. 2025. [Online]. Available: https://www.sciencedirect.com/science/article/pii/S2352484725004366

[12] T. Ravens, "Alaska in-river hydrokinetic energy resources," Tech. Rep., 2014, pp. 1–51.

[13] *Power Cost Equalization Statistical Report FY2023*. Accessed: Oct. 17, 2025. [Online]. Available: https://www.akenergyauthority.org/LinkClick.aspx?fileticket=SjVs3pRjJzrJ8ETEcJzOKQ%3d%3d&portalid=0

[14] (2020). *Renewable Energy ATLAS of Alaska*. [Online]. Available: https://alaskarenewableenergy.org/wp-content/uploads/2020/03/Renewable-Energy-Atlas-2019.pdf

[15] Y.. M. Y. Buswig, A. Affam, A. H. B. Othman, N. B. Julai, Y. S. Sim, and W. M. Utomo, "Sizing of a hybrid photovoltaic-hydrokinetic turbine renewable energy system in east Malaysia," in *Proc. 13th Int. UNIMAS Eng. Conf. (EnCon)*, Oct. 2020, pp. 1–8. [Online]. Available: https://ieeexplore.ieee.org/document/9299329

[16] T. K. Wee, M. Anyi, and N. S. Song, "Small-scale horizontal axis hydrokinetic turbine as alternative for remote community electrification in sarawak," in *Proc. Int. Conf. Smart Grid Clean Energy Technol. (ICSGCE)*, Oct. 2020, pp. 131–136. [Online]. Available: https://ieeexplore.ieee.org/document/9275631

[17] A. Vajari, S. Kotian, S. Shirinnezhad, and D. Ghahremanlou, "Optimizing hybrid energy systems for sustainable development in the Canadian Arctic: A case study of arviat, Nunavut," *J. Urban Dev. Manag.*, vol. 3, no. 3, pp. 150–163, 2024.

[18] P. C. McKinle, M. Wilber, and E. Whitney. (2025). *Learning From Arctic Microgrids: Cost and Resiliency Projections for Renewable Energy Expansion With Hydrogen and Battery Storage*. [Online]. Available: https://www.mdpi.com/2071-1050/17/13/5996

[19] O. Erdinc and M. Uzunoglu, "Optimum design of hybrid renewable energy systems: Overview of different approaches," *Renew. Sustain. Energy Rev.*, vol. 16, no. 3, pp. 1412–1425, Apr. 2012. [Online]. Available: https://linkinghub.elsevier.com/retrieve/pii/S1364032111005478

[20] I. Das and C. A. Cañizares, "Renewable energy integration in diesel-based microgrids at the Canadian Arctic," *Proc. IEEE*, vol. 107, no. 9, pp. 1838–1856, Sep. 2019.

[21] S. Barakat, A. Emam, and M. M. Samy, "Investigating grid-connected green power systems' energy storage solutions in the event of frequent blackouts," *Energy Rep.*, vol. 8, pp. 5177–5191, Nov. 2022. [Online]. Available: https://www.sciencedirect.com/science/article/pii/S2352484722007569

[22] *Modified Kinetic Battery*. Accessed: Jul. 15, 2025. [Online]. Available: https://www.homerenergy.com/products/pro/docs/3.15/modifiedkineticbattery.html

[23] J. Manwell, J. Mcgowan, U. Abdulwahid, and K. Wu, "Improvements to the hybrid2 battery model," in *Proc. Windpower Conf.*, 2025, pp. 1–22.

[24] N. DiOrio, A. Dobos, S. Janzou, A. Nelson, and B. Lundstrom. *Technoeconomic Modeling of Battery Energy Storage in SAM*. Accessed: Jul. 15, 2025. [Online]. Available: http://www.osti.gov/servlets/purl/1225314/

[25] D.-I. Stroe, V. Knap, M. Swierczynski, A.-I. Stroe, and R. Teodorescu, "Operation of a grid-connected lithium-ion battery energy storage system for primary frequency regulation: A battery lifetime perspective," *IEEE Trans. Ind. Appl.*, vol. 53, no. 1, pp. 430–438, Jan. 2017.

[26] K. Smith, A. Saxon, M. Keyser, B. Lundstrom, Z. Cao, and A. Roc, "Life prediction model for grid-connected Li-ion battery energy storage system," in *Proc. Amer. Control Conf. (ACC)*, May 2017, pp. 4062–4068.

[27] *PVGIS User Manual*. Accessed: Jul. 15, 2025. [Online]. Available: https://joint-research-centre.ec.europa.eu/photovoltaic-geographical-information-system-pvgis/getting-started-pvgis/pvgis-user-manualen

[28] T. Huld, E. Paietta, P. Zangheri, and I. Pinedo Pascua, "Assembling typical meteorological year data sets for building energy performance using reanalysis and satellite-based data," *Atmosphere*, vol. 9, no. 2, p. 53, Feb. 2018. [Online]. Available: https://www.mdpi.com/2073-4433/9/2/53

[29] C. Pike, D. Riley, H. Toal, and L. Burnham, "Presenting a model to predict changing snow albedo for improving photovoltaic performance simulation," *Solar*, vol. 4, no. 3, pp. 422–439, Aug. 2024. [Online]. Available: https://www.mdpi.com/2673-9941/4/3/19

[30] T. Ravens, "Site investigaiton report: Hydrokinetic energy assessment of the Yukon river at galena, AK," Univ. Alaska Anchorage, Anchorage, Alaska, Tech. Rep. 1, 2014.

[31] *Monitoring Location Yukon R at Galena AK*. Accessed: Oct. 2, 2025. [Online]. Available: https://waterdata.usgs.gov/monitoring-location/USGS-15564860/
[32] D. Feng, C. J. Gleason, P. Lin, X. Yang, M. Pan, and Y. Ishitsuka, "Recent changes to Arctic river discharge," *Nature Commun.*, vol. 12, no. 1, p. 6917, Nov. 2021. [Online]. Available: https://www.nature.com/articles/s41467-021-27228-1
[33] *Modified Kinetic Battery Model*. Accessed: Oct. 15, 2025. [Online]. Available: https://support.ul-renewables.com/homer-manual-pro/modifiedkineticbatterymodel.html
[34] J. Neubauer. *Battery Lifetime Analysis and Simulation Tool (BLAST) Documentation*. Accessed: Oct. 14, 2025. [Online]. Available: https://www.osti.gov/biblio/1167066
[35] K. Smith, M. Earleywine, E. Wood, J. Neubauer, and A. Pesaran, "Comparison of plug-in hybrid electric vehicle battery life across geographies and drive cycles," in *Proc. SAE Tech. Paper Ser.*, vol. 1, Apr. 2012, pp. 1–11.
[36] Y. Bao, W. Dong, and D. Wang, "Online internal resistance measurement application in lithium ion battery capacity and state of charge estimation," *Energies*, vol. 11, no. 5, p. 1073, Apr. 2018. [Online]. Available: https://www.mdpi.com/1996-1073/11/5/1073
[37] C. Strange, S. Li, R. Gilchrist, and G. dos Reis, "Elbows of internal resistance rise curves in Li-ion cells," *Energies*, vol. 14, no. 4, p. 1206, 2021. [Online]. Available: https://www.mdpi.com/1996-1073/14/4/1206
[38] W. Olis, "Impact of extreme weather on sizing battery energy storage systems: A case study of fairbanks, Alaska," in *Proc. IEEE Electr. Energy Storage Appl. Technol. Conf. (EESAT)*, Nov. 2022, pp. 1–5. [Online]. Available: https://ieeexplore.ieee.org/document/9998028
[39] P. A. Bieniek et al., "Climate divisions for Alaska based on objective methods," *J. Appl. Meteorol. Climatol.*, vol. 51, no. 7, pp. 1276–1289, Jul. 2012. [Online]. Available: https://journals.ametsoc.org/view/journals/apme/51/7/jamc-d-11-0168.1.xml
[40] V. Neary et al., "Methodology for design and economic analysis of marine energy conversion (MEC) technologies," Sandia Nat. Laboratories, Albuquerque, NM, USA, Tech. Rep. SAND2014-9040, 2024.
[41] M. Wilber, E. Whitney, C. Pike, and J. Johnston, "Catching the midnight sun: Performance and cost of solar photovoltaic technology in Alaska," in *Proc. IEEE 46th Photovoltaic Specialists Conf. (PVSC)*, Jun. 2019, pp. 1656–1662. [Online]. Available: https://ieeexplore.ieee.org/document/8980955/
[42] J. Spore. *How to Use the Consumer Price Index (CPI)*. Accessed: Jul. 15, 2025. [Online]. Available: https://dof.ca.gov/media/docs/forecasting/economics/economic-indicators/inflation/How-To-Use-CPI-Data.pdf
[43] *Consumer Price Index*. Accessed: Jul. 15, 2025. [Online]. Available: https://www.minneapolisfed.org/about-us/monetary-policy/inflation-calculator/consumer-price-index-1913-
[44] R. D. Trevizan, A. J. Headley, R. Geer, S. Atcitty, and I. Gyuk, "Integration of energy storage with diesel generation in remote communities," *MRS Energy Sustainability*, vol. 8, no. 2, pp. 57–74, Sep. 2021, doi: 10.1557/s43581-021-00013-9.
[45] J. VanderMeer, M. Mueller-Stoffels, and E. Whitney, "An Alaska case study: Energy storage technologies," *J. Renew. Sustain. Energy*, vol. 9, no. 6, Nov. 2017, Art. no. 061708, doi: 10.1063/1.4986580.
[46] *AEDG–Community–Galena*. Accessed: Apr. 20, 2026. [Online]. Available: https://akenergygateway.alaska.edu/explore/communities/galena/general

BAXTER W. BOND (Member, IEEE) received the B.A. degree in Yup'ik (his heritage language) and the B.S. degree in mechanical engineering from the University of Alaska Fairbanks (UAF), Fairbanks, AK, USA, in 2017 and 2018, respectively. He is currently pursuing the degree in electrical engineering (power systems in rural and remote Alaska). He is also a Researcher with Alaska Center for Energy and Power (ACEP), UAF.

LUKE O. WOODHOUSE received the B.S. degree in mechanical engineering from the University of California, Los Angeles, in 2024. In Summer 2024, he was a Postgraduate Intern with the National Renewable Energy Laboratory, Fairbanks, AK, USA, before joining Alaska Center for Energy and Power (ACEP) in late 2024. His research interests include hydrokinetic resource assessments, debris mitigation, and field testing of turbines.

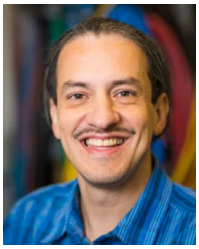

PAUL X. DUVOY is currently a Research Engineer at Alaska Center for Energy and Power (ACEP), University of Alaska Fairbanks (UAF). His work focuses on numerical and analytical modeling for hydrokinetic resources assessment and debris mitigation, open channel hydraulics, marine and river surveying, uncrewed aerial vehicle photogrammetry for mapping and 3-D modeling, field measurements, and data analysis. He has also conducted research modeling for discrete element simulation of geotechnical problems on Mars and the Moon at the UAF Institute of Northern Engineering.

NATHAN J. GREEN received the B.S. degree in applied physics from the University of California, Santa Cruz, Santa Cruz, CA, USA, in 2010, and the M.S. degree in electrical engineering from the University of Alaska Fairbanks (UAF), in 2019. As a Research Professional at Alaska Center for Energy and Power, he has worked on many projects related to Alaska microgrids, including diesel generator economics, low-temperature geothermal power generation, and high-renewable penetration microgrid modeling.

BENJAMIN H. LOEFFLER received the B.S. and M.S. degrees in mechanical engineering from Georgia Institute of Technology, Atlanta, GA, USA. Since 2019, he has worked on riverine hydrokinetic research in Alaska with a focus on field testing turbines and debris mitigation systems at UAF's Tanana River Test Site.